Published in: J. Appl. Phys. **104**, 093107 (2008) / DOI 10.1063/1.3013446

Hybrid CdZnO/GaN quantum-well light emitting diodes

J. W. Mares[1], M. Falanga[1], A. V. Thompson[1], A. Osinsky[2], J. Q. Xie[2], B. Hertog[2], A. Dabiran[2], P. P. Chow[2], S. Karpov[3], and W. V. Schoenfeld[1,*]

[1] CREOL: College of Optics and Photonics, University of Central Florida, Orlando, Florida 32816, USA
[2] SVT Associates, Inc., Eden Prairie, Minnesota 55344, USA
3 STR, Inc., P.O. Box 70604, Richmond, Virginia 23255, USA

Received 11 March 2008, accepted 24 September 2008
Published online 10 November 2008

We report on the demonstration of light emission from hybrid CdZnO quantum-well light emitting diodes. A one-dimensional drift-diffusion method was used to model the expected band structure and carrier injection in the device, demonstrating the potential for 90% internal quantum efficiency when a CdZnO quantum well is used. Fabricated devices produced visible electroluminescence that was found to redshift from 3.32 to 3.15 eV as the forward current was increased from 20 to 40 mA. A further increase in the forward current to 50 mA resulted in a saturation of the redshift.

Preprint (2008)

1 Introduction

ZnO-based compounds have recently gained considerable attention from the scientific community due to the interest in providing an alternative semiconductor material capable of efficient light emission and detection in the UV/visible region. Compared to III-nitride semiconductors, the most compelling advantages of ZnO-based compounds are (i) their large exciton binding energy [1–3] _roughly twice that of GaN), (ii) the commercial availability of native low-dislocation ZnO substrates [4,5] and (iii) their compatibility with both wet chemical and dry etching [6–9]. Furthermore, wurtzite MgZnO and CdZnO alloys with energy band gaps varying from ~1.7 to ~4 eV have been demonstrated [10–16] making such ZnO-based alloys suitable for providing the carrier confinement needed within the active regions of light emitters. However, development of the ZnO-based light emitting devices has been largely impeded by the lack of reliable and stable *p*-doping [17–19]. In order to overcome this current obstacle, hybrid devices containing p-layers made from III-nitride semiconductors and n-layers made from II-oxide alloys have been recently suggested [20,21]. The success in fabrication of hybrid light emitting diodes (LEDs) is largely due to a small (~1.9%) lattice mismatch between ZnO and GaN, allowing a high quality ZnO/GaN interface. However, most hybrid LEDs with ZnO active regions suffer from electron leakage in the *p*-layers of LED structures [22]. The leakage can be partly suppressed in MgZnO/ZnO/III-N double heterostructures, but LEDs with CdZnO active regions have been predicted to offer greater electron confinement [23]. As a result, the internal quantum efficiency (IQE) of such LEDs is expected to be higher, even under high-temperature operation.

In this paper we report on the first demonstration of a hybrid GaN/CdZnO LED, grown using plasma-enhanced molecular beam epitaxy (MBE). A simulation-based analysis of the LED operation was undertaken with the goal of assisting in the analysis of the observed luminescence.

* Corresponding author: winston@creol.ucf.edu

Published in: J. Appl. Phys. **104**, 093107 (2008) / DOI 10.1063/1.3013446

2 LED fabrication and characterization

In this study, we employed a hybrid LED structure consisting of a 300 nm *p*-type GaN spreading layer ($p \sim 7\times10^{17}$ cm^{-3}), an unintentionally doped $Cd_{0.12}Zn_{0.88}O$ single quantum well (QW), a 200 nm *n*-type $Mg_{0.12}Zn_{0.88}O$ confinement layer doped with gallium ($n \sim 1\times10^{17}$ cm^{-3}), and a 15 nm n^+-ZnO contact layer ($n = 5\times10^{18}$ cm^{-3}). The structure was grown by plasma-enhanced MBE on a (0001) sapphire substrate with a pre-existing *p*-GaN layer, providing a high quality *p*-type template for CdZnO LED growth. Based on the growth calibration of thick CdZnO layers directly on sapphire, the $Cd_{0.12}Zn_{0.88}O$ QW thickness was expected to be ~3 nm. However, as discussed below, the growth of strained $Cd_{0.12}Zn_{0.88}O$ on *p*-GaN may have resulted in a smaller QW layer thickness.

Fabrication of the structure was carried out using standard lithographic processes to form the mesa and metal contacts to the *n*- and *p*-regions. First, the LED device mesa (350×350 μm^2) was patterned, exposed, and developed. A 5% HCl/H_2O solution was then used to etch the isolation mesas down to the *p*-type GaN region. It is worth noting that the ability to selectively wet etch the upper *n*-type MgZnO and $Cd_{0.12}Zn_{0.88}O$ QW while leaving the underlying *p*-type GaN layer in tact represents a unique advantage of the hybrid light emitting devices since it is self-limiting. Tapping-mode atomic force microscope (AFM) images of the etched mesa demonstrated the extremely abrupt nature of the natural wet etch stop at the *p*-GaN interface. An interesting feature of the AFM data was the sloped sidewall of the mesa. A line scan from the AFM image revealing a sidewall slope angle of roughly 25° indicates that lateral etching of the ZnO-based top layers occurs faster than vertical etching by a factor of 2. Nonetheless, the in-plane 90° corner angle of the mesa pattern was preserved. The metal contacts were then lithographically patterned for metal deposition. The contact metals were deposited by electron beam evaporation using a Temescal e-beam evaporator, which was followed by a standard metal lift-off procedure. A Ni/Au (10 nm/200 nm) metallization was used to form the contact to *p*-GaN and a Ti/Au (20 nm/200 nm) scheme was applied for the contacts to n^+-ZnO. The samples were then annealed in nitrogen using rapid thermal annealing at a temperature of 420°C for 2 min to increase the Ohmic contact quality. *I-V* characteristics taken from the devices verified a rectifying behavior; however, it was observed that higher contact annealing temperature resulted in degradation of the rectifying behavior, thus limiting the annealing temperature that could be used. The quality of the lithography was found to be very high and to be of equal quality with that attained on III-nitride LEDs.

The LED structures and die were characterized by both photoluminescence (PL) and electroluminescence (EL) measurements. PL measurements were carried out with a He-Cd laser (λ_e = 325 nm)_ in cw mode with a pump power density of 10 kW/cm^2. EL was measured under constant current from the top of the die. Light was collected with a 10× objective lens and directed into a Newport MS257 spectrometer attached with a cooled silicon charge coupled device (CCD) camera. An optical image of a fabricated LED die operating at a current of 50 mA is shown in Fig. 1. Clear emission of blue light from the hybrid LED is observed. Due to the sloped mesa sidewalls, light emission appears enhanced at the edges of the mesa, as can be seen in the image.

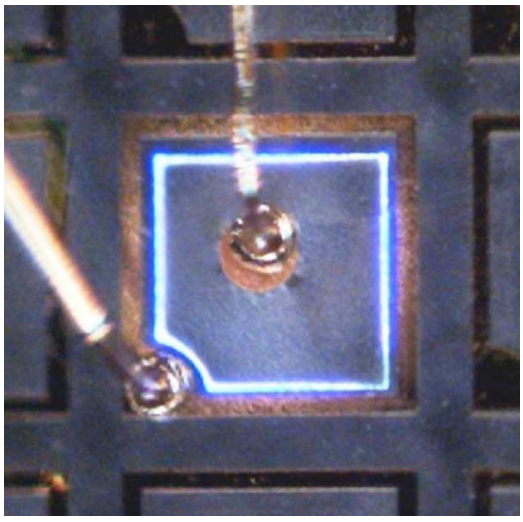

Fig. 1 Photograph of an operating 350×350 μm^2 hybrid LED die under 50 mA forward bias.

PL measurements showed strong luminescence centered at 430 nm with a full width at half maximum (FWHM) of ~90 nm [see Fig. 2(a))]. No measurable low-energy defect luminescence was observed. The measured EL spectra of the hybrid LED are shown in Fig. 2(b) for forward currents varying from 20 to 50 mA. Consistent with the PL spectra, we did not observe any significant defect luminescence bands in the EL emission, indicative

of the high quality growth. The EL peak wavelength was observed to redshift from 390 nm at 20 mA to 410 nm at 40 mA. This was followed by a very slight blueshift to 407 nm when the current was increased to 50 mA. The FWHM of the EL reached a maximum of ~43 nm between 30 and 40 mA and was in the range 34-37 nm for 20 and 50 mA. The origin of the observed PL and EL will be discussed in the next section.

3 Analysis of LED operation

To explore the possible benefits of using a CdZnO active region, we modeled the hybrid LED operation. The simulations were made with the SILENSE 3.4 package [24] that combines a one-dimensional drift-diffusion approach for carrier transport with a quantum-mechanical calculation of the light emission spectra. Both spontaneous and piezopolarization of all wurtzite materials were accounted for in the simulations to predict properly the electric potential distribution in the LED structure. The electron concentration in the unintentionally doped CdZnO QW was assumed to be ~10^{17} cm^{-3}, though its value was checked to weakly affect the modeling results. Radiative recombination of electrons and holes and nonradiative carrier recombination at threading dislocations, corresponding to the dislocation density of ~10^9 /cm^2, were considered as principal recombination mechanisms. Specific details of the simulation model can be found in Ref.[25]. The chosen threading dislocation density (TDD) is typical for GaN grown on sapphire by both metal-organic chemicalvapor deposition and MBE. The fact that TDD in II-oxide epitaxial materials does not exceed that of the GaN template has been proven in Ref.[26]. We do not consider here the possible nonradiative carrier recombination via interface defects since apparent observation of tunnel radiative recombination in various hybrid heterostructures suggests high quality of the II-oxide oxide/III-nitride interfaces (see discussion of this issue in Ref.[22]).

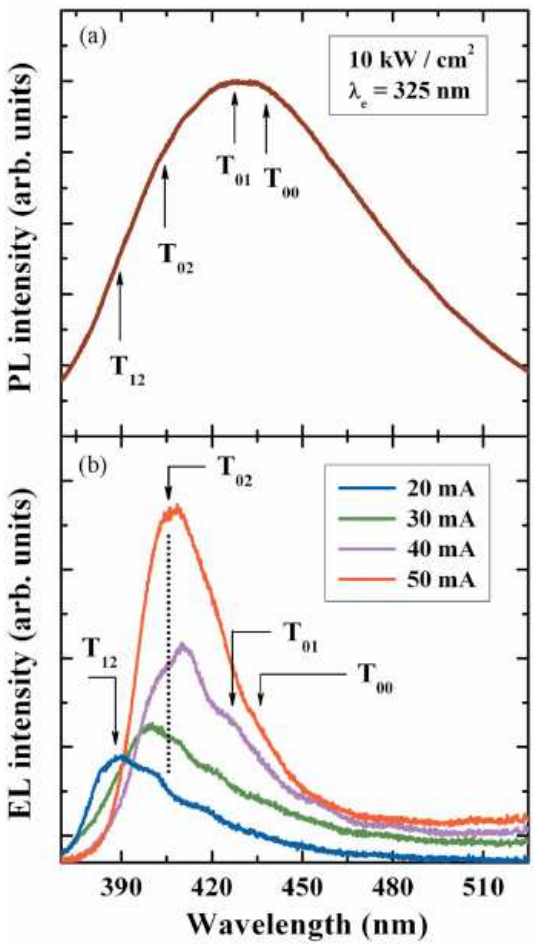

Fig. 2 Measured (a) PL and (b) EL spectra of a hybrid LED at various forward currents. Arrows indicate principal optical transitions calculated for the LED with a 1.2 nm $Cd_{0.12}Zn_{0.88}O$ QW.

As shown previously [21,22], the type-II band alignment at the GaN/CdZnO interface implies that both spatially direct recombination between electrons and holes in the CdZnO QW and spatially indirect (or tunnelling) recombination of the CdZnO QW electrons with holes trapped at the GaN/CdZnO interface may occur in the hybrid LED structure. To assess the role of each of these recombination channels we calculated the emission spectra with and without the tunneling emission taken into account. A uniform broadening of 50 meV for the emission line Γ was used in the simulations. This value was based on the measured decay of the shortwavelength wings of the EL spectra.

Figure 3(a) plots the computed dependence of the peak emission wavelength on the computed $Cd_{0.12}Zn_{0.88}O$ QW width for the case when spatially indirect carrier recombination is taken into account

(solid blue line) and for the case when it is not (dashed green line). The peak wavelength of the spectra for the first case clearly shows a sharp drop at a critical QW width of 2.55 nm. This transition is accompanied by the appearance of the spatially direct recombination peak in the spectrum, which dominates for wide enough QW (see spectra in the Fig. 3(a) insets). The peak wavelength may actually vary between the blue and green curves in Fig. 3_a_ because of competition between the spatially direct and indirect recombination mechanisms. The contribution of each mechanism to the light emission may depend not only on the forward current but also on the difference in the yield of these recombination mechanisms. This latter factor could not be accounted for in the simulations, however.

The emission wavelength from bulk $Cd_{0.12}Zn_{0.88}O$ is expected to peak at 425-430 nm [14]. Excitonic effects should only result in a longer wavelength emission rather than the much shorter (~390-410 nm) peak wavelength obtained in our EL measurements. We attribute this blueshift to quantum confinement effects in the CdZnO QW. Despite the targeted 3 nm QW width, the theoretical predictions become consistent with the measured EL peak wavelengths if it is assumed that the QW width is ~1.0-1.2 nm. This smaller QW thickness, as compared with that expected from the growth rate calibration, may originate from the strain in CdZnO coherently grown on p-GaN template, generally increasing the material free energy and thus reducing its growth rate. Figure 3(b) compares the theoretical and experimental dependences of the peak EL emission wavelength on forward current of the hybrid LED. The theory predicts a relatively weak blueshift with the current density for both spatially direct and indirect light emissions. In contrast, the experimental points demonstrate a redshift with increasing current that we attribute to competition of the two recombination channels (direct and indirect). From comparison of the theory with measurements we can conclude that the role of the spatially indirect recombination increases with forward current. A more detailed analysis of the direct and indirect optical transitions will be given below.

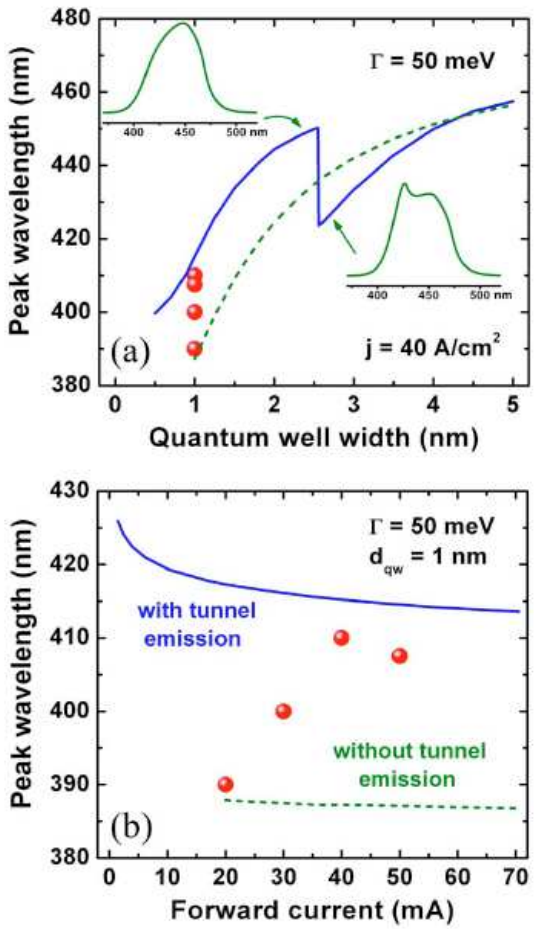

Fig. 3 (a) Peak emission wavelength vs $Cd_{0.12}Zn_{0.88}O$ QW width calculated with (solid blue line) and without (dashed green line) spatially indirect (tunnel) carrier recombination taken into account. (b) Peak emission wavelength as a function of foward current in the hybrid LED structure with a 1.0 nm $Cd_{0.12}Zn_{0.88}O$ QW. Circles indicate the experimental peak wavelength positions obtained at different forward currents. Insets in (a) demonstrate the change in the emission spectra below and above the transition point.

The room-temperature band diagram and distributions of electron and hole concentrations in the LED structure with a 1.2 nm QW are shown in Fig. 4(a) for the case when the current density is 40 A/cm^2 (this current density nearly corresponds to the forward current of 40 mA). The concentration of electrons injected into the $Cd_{0.12}Zn_{0.88}O$ QW can be seen to be high enough for efficient emission despite only a moderate doping of the *n*-MgZnO cladding layer, a result of the superinjection effect. In contrast, the hole concentration in the well is considerably lower than in the *p*-GaN contact layer. This is due to type-II band alignment and the resulting potential barrier for holes formed at the GaN/CdZnO interface. The hole concentration is found, nevertheless, to be sufficient to confine radiative recombination to the

$Cd_{0.12}Zn_{0.88}O$ QW. The electron and hole leakages are predicted to remain low for current densities up to ~2–3 kA/cm^2 and operating temperatures up to 125 °C. The latter provides evidence of a potential benefit resulting from the use of a CdZnO active region. In determining the IQE it was assumed that the nonradiative carrier recombination results from threading dislocations with a density of 10^9 /cm2. The estimated IQE of the hybrid LED was then determined to be _90% at room temperature and ~80% at 125°C, results that are nearly independent of the current density. This correlates with the conclusion made in Ref.[23] that a CdZnO active region should lead to considerable improvement in the LED performance.

Figure 4(b) shows the wave functions of electron and hole states computed for the hybrid CdZnO LED structure. The electron level denoted as "e_0" corresponds to the ground-state wave function confined in the CdZnO QW. The wave function of the next level "e_1" spreads considerably in the MgZnO layer. There are, in addition, more than 40 other electron levels lying slightly above e_1 and oscillating near the CdZnO/MgZnO interface. In contrast, only three main hole states were predicted for the hybrid LED structure. The double-degenerate level "h_0" corresponds to heavy and light holes localized in the *p*-GaN layer near the GaN/CdZnO interface. The level "h_1" belongs to ground-state split-off holes also in the p-GaN layer. Only the double-degenerate level "h_2" is related to the heavy and light holes confined in the CdZnO QW. Since holes at this level can potentially penetrate into the *p*-GaN by tunneling, the level h_2 is actually just a resonance state.

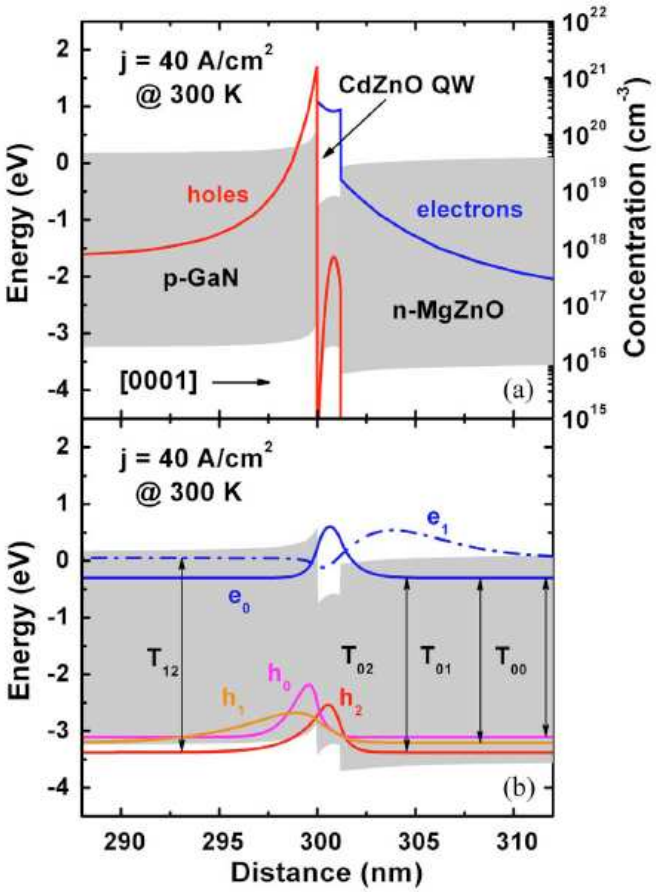

Fig. 4 Simulation results for the hybrid LED with a 1.2 nm $Cd_{0.12}Zn_{0.88}O$ QW operating at the current density of 40 A/cm^2. (a) Band diagram and distributions of carrier concentrations and (b) wave functions of electrons (blue lines) and holes (orange, magenta, and red lines) near the QW and principal optical transitions.

Figure 4(b) also shows the possible optical transitions T_{jk} that may occur, i.e., the transitions from the electron level "e_j" to the hole level "h_k." The transition T_{02} is the most likely to occur since, at 0.89, it has the largest square overlap integral between the electron and hole wave functions for the carriers confined in the QW. The transitions T_{00} and T_{01} are much less likely since their square overlap integrals have values of 0.16 and 0.15, respectively. However, they may still contribute significantly to the emission spectrum since the concentration of holes adjacent to the GaN/CdZnO interface (~10^{21} cm^{-3}) is much higher than the hole concentration in the QW (~10^{18} cm^{-3}) as can be seen from Fig. 4(a). The transition T_{12}, involving the excited electron state e_1, has the lowest probability with square overlap integrals near 0.01.

The above analysis clearly shows that the luminescence spectra of the hybrid LED structure are determined by competition of the spatially direct recombination between electrons and holes in the CdZnO QW (T_{02} and T_{12} transitions) and spatially indirect (or tunnelling) recombination of the CdZnO QW electrons with holes trapped at the GaN/CdZnO interface (T_{00} and T_{01} transitions). The spectral positions

of these transitions computed for a $Cd_{0.12}Zn_{0.88}O$ QW width of 1.2 nm are indicated in the measured PL and EL spectra in Fig. 2. One can see that each of the transitions correlates well with some features (peaks and shoulders) observed in the EL spectra. In particular, the peak emission wavelength of ~390 nm corresponds to the less probable T_{12} transition for a forward current of 20 mA. This may be evidence for a significant contribution from the excited electron state e1 to the light emission. Increasing the hole concentration in the QW with current makes the recombination of ground-state electrons and holes dominant, so that the peak emission wavelength redshifts to the position corresponding to the T_{02} transition. In turn, the spatially indirect transitions T_{00} and T_{01} seem to be responsible for the long-wavelength wings of the EL spectra. In any case, light emission is governed at high currents by intrawell recombination of nonequilibrium carriers confined in the CdZnO QW. The competition between different recombination channels under current variation may depend on many factors, including the well thickness, composition fluctuations, the quality of the GaN/CdZnO interface, and strain relaxation. We believe that this competition is responsible for the measured peak wavelength variation with current, showing a strong redshift of the spectra. However, the blueshift observed under the forward current increasing from 40 to 50 mA is in line with the theoretically predicted tunnel _spatially indirect_ emission, perhaps indicating that the emission is at that point dominated by the spatially indirect recombination channel. These issues need further theoretical and experimental work to be clarified.

Figure 2(a) demonstrates a quite different behavior for the PL spectrum. To begin with, the position of the PL peak wavelength corresponds to the spatially indirect transition rather than to the intrawell recombination. Second, there is a long-wavelength wing in the PL spectrum reaching beyond that due to the spatially direct and indirect transitions. This results in an emission spectrum twice as broad as that of the EL. The nature of the long-wavelength wing is not understood and requires further investigation.

4 Conclusion

For the first time we have demonstrated visible EL from a hybrid *n*-MgZnO/CdZnO/*p*-GaN LED heterostructure with a single $Cd_{0.12}Zn_{0.88}O$ QW. EL from the device was found to redshift from 390 to 410 eV as the forward current was increased from 20 to 40 mA. This observation was qualitatively explained in terms competing intrawell optical transitions determined through simulations involving both ground and excited electron states in the QW. Domination of the intrawell emission despite there only being an extremely thin active region in the LED structure provides evidence for advantages of using CdZnO to provide efficient light emission from hybrid LEDs. The measured PL spectrum differs significantly from the EL emission. Unlike the EL spectra, the PL spectrum appears to be due to spatially indirect optical transitions between the electrons confined in the QW and holes accumulated at the GaN/CdZnO interface.

Acknowledgments

The authors would like to acknowledge the support of the Army Research Office under Contract No. W911NF-05-C-0024, monitored by Dr. Michael Gerhold. We would also like to acknowledge valuable discussions with Dr. David Look.

References

[1] D. C. Reynolds, D. C. Look, and B. Jogai, Solid State Commun. **99**, 873 (1996).

[2] D. C. Reynolds, D. C. Look, B. Jogai, and T. C. Collins, Phys. Rev. B **56**, 13753 (1997).

[3] P. Zu, Z. K. Tang, G. K. L. Wong, M. Kawasaki, A. Ohtomo, H. Koinuma, and Y. Segawa, Solid State Commun. **103**, 459 (1997).

[4] D. C. Look, D. C. Reynolds, J. R. Sizelove, R. L. Jones, C. W. Litton, G. Cantwell, and W. C. Harsch, Solid State Commun. **105**, 399 (1998).

[5] M. Suscavage, M. Harris, D. Bliss, P. Yip, S.-Q. Wang, D. Schwall, L. Bouthillette, J. Bailey, M. Callahan, D. C. Look, D. C. Reynolds, R. L. Jones, and C. W. Litton, MRS Internet J. Nitride Semicond. Res. **4S1**, G3.40 (1999).

[6] J. W. Bae, C. H. Jeong, H. K. Kim, K. K. Kim, N. G. Cho, T. Y. Seong, S. J. Park, I. Adesida, and G. Y. Yeom, Jpn. J. Appl. Phys., Part 2 **42**, L535 (2003).

[7] J. J. Chen, S. W. Jang, F. Ren, Y. J. Li, H. S. Kim, D. P. Norton, S. J. Pearton, A. Osinksy, S. N. G. Chu, and J. F. Weaver, J. Electron. Mater. **35**, 516 (2006).

[8] H. K. Kim, J. W. Bae, K. K. Kim, S. J. Park, T. Y. Seong, and I. Adesida, Thin Solid Films **447**, 90 (2004).

[9] K. Takahashi, H. Funakubo, N. Ohashi, and H. Haneda, Thin Solid Films **486**, 42 (2005).

[10] S. Choopun, R. D. Vispute, W. Yang, R. P. Sharma, T. Venkatesan, and H. Shen, Appl. Phys. Lett. **80**, 1529 (2002).

[11] T. Gruber, C. Kirchner, R. Kling, F. Reuss, A. Waag, F. Bertram, D. Forster, J. Christen, and M. Schreck, Appl. Phys. Lett. **83**, 3290 (2003).

[12] S. S. Hullavarad, N. V. Hullavarad, D. E. Pugel, S. Dhar, I. Takeuchi, T. Venkatesan, and R. D. Vispute, J. Phys. D **40**, 4887 (2007).

[13] T. Makino, Y. Segawa, M. Kawasaki, A. Ohtomo, R. Shiroki, K. Tamura, T. Yasuda, and H. Koinuma, Appl. Phys. Lett. **78**, 1237 (2001).

[14] J. W. Mares, F. R. Ruhge, A. V. Thompson, P. G. Kik, A. Osinsky, B. Hertog, A. M. Dabiran, P. P. Chow, and W. V. Schoenfeld, Opt. Mater. (Amsterdam, Neth.) **30**, 346 (2007).

[15] S. Shigemori, A. Nakamura, J. Ishihara, T. Aoki, and J. Temmyo, Jpn. J. Appl. Phys., Part 2 **43**, L1088 (2004).

[16] A. Osinsky and J. Muth, in *Wide Bandgap Light Emitting Materials and Devices*, edited by G. F. Neumark, I. L. Kiskovsky, and H. Jiang (Wiley, Weinheim, Germany, 2007), pp. 179–204.

[17] O. Lopatiuk-Tirpak, W. V. Schoenfeld, L. Chernyak, F. X. Xiu, J. L. Liu, S. Jang, F. Ren, S. J. Pearton, A. Osinsky, and P. Chow, Appl. Phys. Lett. **88**, 202110 (2006).

[18] H. W. Liang, Y. M. Lu, D. Z. Shen, Y. C. Liu, J. F. Yan, C. X. Shan, B. H. Li, Z. Z. Zhang, J. Y. Zhang, and X. W. Fan, Phys. Status Solidi A **202**, 1060 (2005).

[19] D. P. Norton, Y. W. Heo, M. P. Ivill, K. Ip, S. J. Pearton, M. F. Chisholm, and T. Steiner, Mater. Today **7**, 34 (2004).

[20] K. A. Bulashevich, I. Y. Evstratov, V. N. Nabokov, and S. Y. Karpov, Appl. Phys. Lett. **87**, 243502 (2005).

[21] A. Osinsky, J. W. Dong, M. Z. Kauser, B. Hertog, A. M. Dabiran, P. P. Chow, S. J. Pearton, O. Lopatiuk, and L. Chernyak, Appl. Phys. Lett. **85**, 4272 (2004).

[22] A. Osinsky and S. Karpov, in *Zinc Oxide Bulk, Thin Films and Nanostructures: Processing, Properties and Applications*, edited by C. Jagadish and S. J. Pearton (Elsevier, London, 2006), pp. 525–554.

[23] K. A. Bulashevich, I. Y. Evstratov, and S. Y. Karpov, Phys. Status Solidi A **204**, 241 (2007).

[24] see http://www.semitech.us/products/SiLENSe/ for details on the software package.

[25] S. Y. Karpov, in *Nitride Semiconductor Devices: Principles and Simulation*, edited by J. Piprek (Wiley, Weinheim, 2007), p. 303–325.

[26] H. S. Yang, S. Y. Han, Y. W. Heo, K. H. Baik, D. P. Norton, S. J. Pearton, F. Ren, A. Osinsky, J. W. Dong, B. Hertog, A. M. Dabiran, P. P. Chow, L. Chernyak, T. Steiner, C. J. Kao, and G. C. Chi, Jpn. J. Appl. Phys., Part 1 **44**, 7296 (2005).